https://doi.org/10.20965/jdr.2019.p0616

Paper:

A Simple Procedure for Measuring Magma Rheology

Aika K. Kurokawa*,†, Takahiro Miwa*, and Hidemi Ishibashi**

*National Research Institute for Earth Science and Disaster Resilience (NIED)
3-1 Tennodai, Tsukuba, Ibaraki 305-0006, Japan
†Corresponding author, E-mail: kurokawa@bosai.go.jp
**Department of Geosciences, Faculty of Science, Shizuoka University, Shizuoka, Japan
[Received November 1, 2018; accepted February 16, 2019]

In this study, a procedure to measure the viscosity of multi-phase magma at high temperatures (>1000°C) was developed by using a simple apparatus comprising a commercially available desktop furnace and viscometer. In particular, the use of a disposable container enabled observations of the microstructure of an entire sample. The procedure was applied to basaltic andesite magma of the 1986 Izu–Oshima fissure eruption, Japan. The results show that reliable data, consistent with previous studies, were obtained and that the magma rheology became non-Newtonian with decreasing temperature, showing clear shear-thinning behavior. The rheological properties of the magma at 1180°C are quantitatively described as a function of shear rate based on three simple non-Newtonian fluid models. Sectional views of the sample confirm that plagioclase and Fe–Ti oxide crystals were nearly uniformly dispersed in the sample. The mean crystal volume fraction of 0.14 enabled crystal interactions inducing changes in crystal arrangement, affecting the rheology.

Keywords: magma, rheology, non-Newtonian, microstructure, Izu–Oshima

1. Introduction

Rheological properties of multiphase magma composed of melt and crystals and/or bubbles play a fundamental role in magma transport in volcanic conduits and lava flows [1–4]. Given that flows of magma and lava are responsible for the major volcanic hazards, understanding magma rheology is important not only for scientific interest but for disaster mitigation. As such, many studies have experimentally attempted to determine the rheological properties of magma [5, 6].

Experimental methods require measurements of the viscosity of a fluid, and instruments for this purpose are termed viscometers. Various viscometers are used in many fields, such as the food industry [7], cosmetics [8], and soft matter research [9]. In the field of magma rheology, concentric viscometers in which fluid fills a gap between a columnar container and a round bar or rod are often used to measure shear rheology by rotating the rod, although the experimental methods show a remarkable range [5, 10–16]. Compared to other fluids for which rheology can be measured in a narrow temperature range of approximately room temperature, rheological measurements of magma require tight temperature controls. In the case of basalt and basaltic andesite, the temperature needs to be quite high (more than ∼1000°C) to obtain fluid magma, and the crystal volume fraction varies even over slight temperature changes (<10°C). Despite the challenges of obtaining such measurements, previous studies have revealed many rheological characteristics of magma, as summarized by [6]. Most experimental apparatuses in previous studies used platinum containers, which have a higher melting point than that of the magma to minimize reaction with the magma, although reaction with iron is inevitable [5, 10–12, 14–16]. Since platinum containers are expensive and typically reused, many studies have focused on the rheology or observed microstructure directly around the rod, while there are a few pioneering studies that succeeded completing a textural analysis of quenched samples excluding the 1–2 mm thick melt ring at the container wall [15, 16].

This study attempted to perform rheological measurements of basaltic andesite magma using our own experimental apparatus, which has two main advantages. First, the apparatus was made as simply as possible by using a desktop furnace with a door from which the experimental sample can be easily introduced or removed. Second, the use of a disposable container enables observation of the microstructure of an entire sample following each experiment, which might provide a better understanding of the magma flow dynamics. The aim of this study was to develop a procedure for measuring magma rheology that is simple and link the rheological characteristics of magma to microstructure. The experimental sample was a lava produced by the 1986 Izu–Oshima fissure eruption. The remainder of this paper is organized as follows. Section 2 describes the sample and Section 3 provides an outline of the experimental apparatus and protocols. The preparation for rheological measurements and microstructural observations are explained in Section 4. The results of the rheological measurements, followed by a discussion of the rheological characteristics and sample microstructure, are presented in Section 5. Particular focuses of this

Table 1. Major elemental composition of the LB1 experimental sample obtained using X-ray diffraction analysis.

Oxide	[wt.%]
SiO_2	54.95
TiO_2	1.24
Al_2O_3	14.25
FeO	13.96
MnO	0.23
MgO	3.76
CaO	8.67
Na_2O	2.26
K_2O	0.54
P_2O_5	0.13
Total	99.99

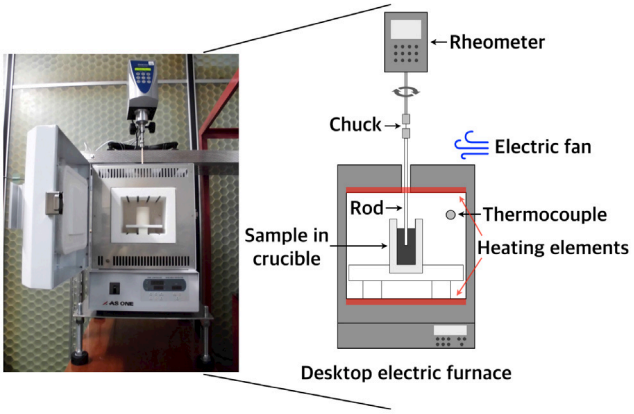

Fig. 1. Photograph and schematic view of the experimental apparatus used in this study.

study were non-Newtonian magma rheology induced by the effect of crystals and demonstrating the veracity of the experimental apparatus and protocols.

2. Material

Izu–Oshima, an island 110 km SSW of Tokyo, is among the most active volcanoes in Japan. An eruption in November 1986 comprised three eruptive episodes at the summit (crater A), fissures in the caldera floor (crater B), and fissures in the flank of the outer rim (crater C) [17]. In this study, lava from the 1986 Izu–Oshima eruption at crater B (LB1) was sampled from the island (34°44′24″N, 139°24′00″E). We chose LB1 as an experimental sample because the lava lacks phenocrysts, thus it can be melted within a relatively short period of time. Moreover, by controlling the temperature between the liquidus and solidus, the effect of microstructural changes in crystals on the rheology were expected to be observed. In addition, the sample was classified as an aphyric basaltic andesite according to the chemical composition provided in **Table 1**, consistent with those of the other LB1 samples collected within one year after the eruption [18, 19]. Given that the melt viscosity of basaltic andesite is lower than that of andesite or rhyolite, various rheological variations can be measured by mass-produced viscometers with low effective measuring torque ranges.

3. Experimental Apparatus

Rheological measurements of the LB1 magma were conducted using our own experimental apparatus with the following features: (1) the apparatus was made as simply as possible for widespread application; and (2) the microstructure of the entire sample in the container was observable following each experiment. The apparatus was designed and constructed as follows.

The apparatus, shown in **Fig. 1**, comprises a concentric cylindrical viscometer (HBDV-II+Pro, Brookfield Engineering Laboratories) connected to an alumina rod introduced into a desktop electric furnace (HPM-0G, AZ ONE) from a hole on the top, similar to the method developed by Sato [5]. The furnace originally had a hole, and heating elements were installed at the top and bottom surfaces. The viscometer determined the shear stress controlling the shear rate. Rheological data were automatically calculated within the viscometer, as the sizes of the crucible container and rod match those of the standard parts for the viscometer. The viscometer converted the angular velocity of the rod (ω) into the shear rate ($\dot{\gamma}$), and the torque (M) into the shear stress (σ) using a container radius of 9.5 mm (R_c), rod radius of 2.5 mm (R_r), and sample height of 15 mm (L) as follows:

$$\dot{\gamma} = \frac{2\omega R_c^2 R_r^2}{x^2(R_c^2 - R_r^2)} \quad \cdots\cdots\cdots\cdots\cdots (1)$$

$$\sigma = \frac{M}{2\pi R_r^2 L} \quad \cdots\cdots\cdots\cdots\cdots (2)$$

where the radius at the which shear rate is calculated (x) is assumed to be 7.8 mm. Although the shear rate could vary given a change in x [20], we assumed x as constant. In any of these cases, the fluid is assumed to be a Newtonian fluid. The viscosity is the shear stress divided by the shear rate. The measurement precision was calibrated using a viscosity standard (oil JS14000) of which the viscosity was 12 Pa·s at 20°C by varying the shear rate. The most elaborate part of the apparatus is the crucible container for the experimental sample. An alumina crucible container with 17% porosity filled with the LB1 sample was placed inside the furnace. The porous crucible, 62 mm in height, was selected to prevent fracturing during water quenching and maximize the quenching rate. Above the furnace, an electric fan prevents heating from the viscometer due to hot gas escape. The components in contact with the sample (i.e., the container and rod) were composed of alumina, as it is inexpensive compared to platinum and has a much higher melting point (2050°C) than that of magma. The reaction between the alumina instruments

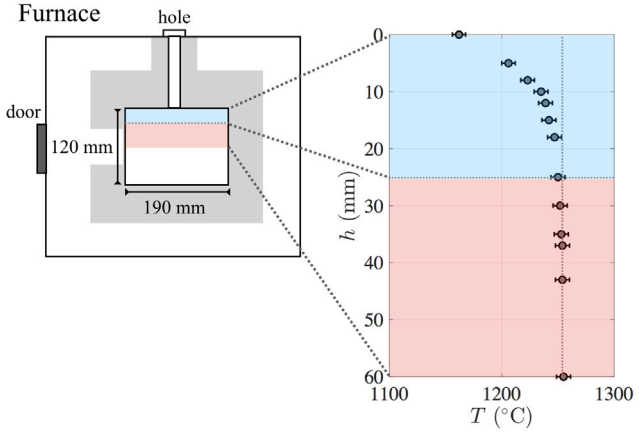

Fig. 2. Vertical temperature distribution in the furnace at a set temperature of 1250°C.

and experimental sample in this study was insignificant, as demonstrated in Section 5.3. The alumina instruments were designed in-house to fit the viscometer and furnace, and custom-made by Hashimoto Riken Kogyo. The use of disposable items allowed microstructural observation of the entire sample from a variety of orientations by cutting the quenched sample and container.

The cylindrical furnaces used in previous studies maintain a constant temperature [21], whereas the temperature in our desktop furnace was unclear. Therefore, the vertical distribution of temperature inside the furnace below the hole on the top of the apparatus was measured using a K-type thermocouple (Sakaguchi E.H VOC Corp.), because the sample container and rod were aligned below the hole. As shown in **Fig. 2**, temperature stability in the furnace was confirmed, apart from the upper side from the top to 24 mm depth. Although temperatures at $h > 60$ mm could not be directly measured because of the thermocouple length, these would be stable as the lower part is the most distant from the top hole, and heating elements were installed not only at the top surface but also at the bottom surface. Similarly, the sample temperature was considered to be stable and controllable because the height of the sample was approximately 40 mm $\leq h \leq$ 80 mm in the central area of the furnace.

4. Sample Preparation

4.1. Rheological Measurements

For rheological measurements, the sample was washed and crushed to a particle size less than 4 mm. The particles were neither powdered nor isometric, as this facilitates smooth degassing and melting; i.e., if powdery particles are rigidly packed in an orderly manner, it takes much more time to remove bubbles via stirring. In contrast, the gas percolation rate through the spaces between the particles increases with increasing particle size. A container of LB1 particles was set on an alumina stand on ceramic wool and platinum wire was placed in the furnace such that the rod inserted into the furnace hole was situated at the very center of the crucible. To completely melt the sample, the temperature in the furnace increased and held for two days at 1260°C, which was determined in consideration of the upper temperature limit of the furnace. During the middle of the melting process, the rod was inserted into the sample and the fluid was weakly stirred at a shear rate of 1.1 s^{-1} to promote degassing and homogenization. Subsequently, the temperature was set to the experimental temperature for at least one day prior to the rheological experiments to allow time for crystallization and stabilization. After these steps, two types of shear-rate-controlled tests were undertaken. One was a shear rate sweeping test at various temperatures and the other was a constant shear rate test at 1180°C. Prior to the measurements, pre-shearing was applied at 7.7 s^{-1} for 5 min to initialize the sample. All experiments were conducted in an atmospheric environment and at ambient pressure. Oxygen-fugacity-controlled experiments can also be conducted using this apparatus via gas injection through a vent [5, 14]. However, such studies are a subject of future research.

4.2. Microstructural Observations

Microstructural observations of the sample in the container were required to examine the effect of crystals on the rheology. To observe the microstructure, the rod was gently extracted from the crucible, and the sample was immediately quenched in water after measurements. The quenched sample was mounted in resin (Petropoxy 154, Palouse Petro Products) and carefully polished for observations using scanning electron microscopy (JSM-6610, JEOL).

5. Results and Discussion

5.1. Shear Rate Sweeping Test

Shear rate sweeping tests were performed by continuously increasing the shear rate from 1 s^{-1} to 16 s^{-1} and back down at temperatures of 1180, 1200, and 1235°C. The temperatures were selected considering the temperature limit of the furnace and the torque limit of the viscometer. Measurement of each shear rate was undertaken for 5 min which is longer than the relaxation time in all cases, although the relaxation time increases with a decreasing shear rate and temperature. The series of experiments was conducted three times and the reproducibility was confirmed. After all the experiments, the sample was extracted from the furnace and quenched at 1180°C. As shown in **Fig. 3**, the results were compared to a multicomponent chemical model for predicting the viscosity of silicate melts, as proposed by [22]. At 1235°C, the measured viscosity, which does not depend on the shear rate, is approximately the same as that estimated by the model. Given that the model only considers silicate melts, this result means that the sample did not contain crystals at

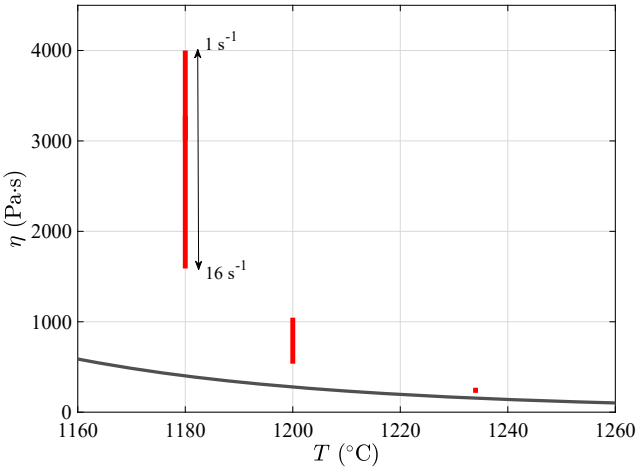

Fig. 3. Relationship between viscosity (η) and temperature (T). Red lines indicate the viscosity range obtained using the by shear rate sweeping tests, whereas the black line is a model for silicate melt using the data shown in **Table 1** [22]. As indicated by the arrow at 1180°C, the maximum and minimum viscosities were measured at shear rates of 1 s^{-1} and 16 s^{-1} at each temperature, respectively.

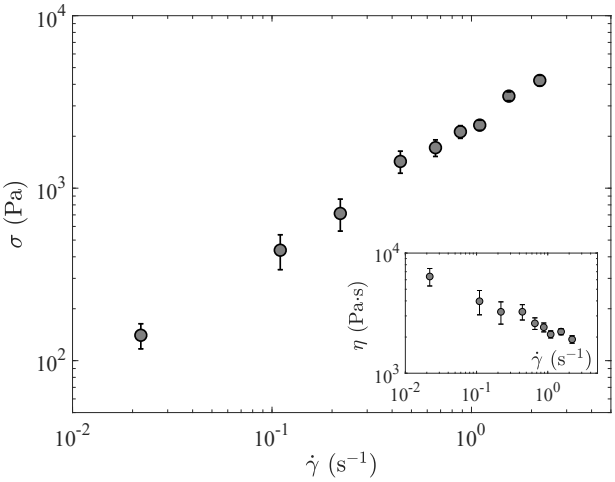

Fig. 4. Relationship between shear stress (σ) and shear rate ($\dot{\gamma}$) at steady state. The filled circles indicate the average value of shear stress measured during the last 1 min and the error bar is the standard deviation. The inset shows the relationship between viscosity (η) and shear rate ($\dot{\gamma}$).

this temperature. In fact, we confirmed that the quenched sample was crystal-free using textural analysis. Even if it slightly contains crystals, the measured viscosity of the sample is regarded as the melt viscosity since the effect of a small amount of crystals on bulk viscosity is negligible [6]. The consistency between the experimental result and model justifies the validity of our method, allowing it to be used for other magma rheology measurements.

However, the measured viscosity deviates from the model (i.e., it is higher and shear-rate dependent) at lower temperatures because of the effect of crystallization. This effect becomes more apparent with decreasing temperature, or with an increasing crystal volume fraction.

5.2. Constant Shear Rate Test

As shown in **Fig. 3**, the viscosity varies with shear rate because of the interaction between crystals at 1180 and 1200°C [14]. Here, we provide more detail regarding the shear rate dependence at a temperature of 1180°C, as derived from the constant shear rate test. During the experiment, the sample was subjected to a constant shear for longer than 30 min after the shear stress became nearly constant. **Fig. 4** shows that the relationship between the shear stress and shear rate is linear in a double logarithmic plot at the steady state, and that the viscosity decreases with increasing shear rate, which is referred to as shear thinning. Given that shear thinning has been observed in many different magmatic systems composed of melt and crystals (e.g. [3, 23]), it is a common characteristic caused by crystal–melt interactions. However, the type of crystals in the sample should be identified to examine the interactions in detail.

The relationship between the shear stress and shear rate shown in **Fig. 4** was then fitted to three representative non-Newtonian fluid models as follows:

Hershel–Bulkley (HB) model:

$$\sigma = K \cdot \dot{\gamma}^n + \sigma_0 \quad \ldots\ldots\ldots\ldots\ldots\ldots \quad (3)$$

Bingham model:

$$\sigma = \eta_B \cdot \dot{\gamma} + \sigma_0 \quad \ldots\ldots\ldots\ldots\ldots\ldots \quad (4)$$

Power-law (PL) model:

$$\sigma = K \cdot \dot{\gamma}^n \quad \ldots\ldots\ldots\ldots\ldots\ldots \quad (5)$$

where σ is the shear stress, K is the consistency index, η_B is the Bingham viscosity, $\dot{\gamma}$ is the shear rate, n is the flow index, and σ_0 is the yield stress. The parameters of the three models are listed in **Table 2** with the root-mean square error (RMSE). The HB and PL models fit well to the data with a similar RMSE, whereas the Bingham model has a higher RMSE. The difference in fit is clearly shown in **Fig. 5**. Similarly, the K and n values of the HB and PL models are nearly the same. The n value of 0.75 means that the sample is a shear-thinning fluid, which is also consistent with the inset in **Fig. 4**. However, the yield stresses estimated by the HB and Bingham models are different. A larger yield stress was estimated by the Bingham model, as it does not consider the shear-thinning nature of the sample. In addition, it is evident in **Fig. 5** that the Bingham model does not capture the measured rheology at low shear rates (e.g., < 0.2 s^{-1}) causing an artifact. Given that the sample is a shear-thinning fluid, we discuss the results of the HB model, which considers shear thinning and yield stress. Because the HB model describes the rheological characteristics at a steady state, the result of $\sigma_0 = 3.1$ Pa indicates that the yield stress is sufficiently small to be ignored after reaching the steady state. This means that simulation of steady state magmatic flow can be simplified without considering the yield stress. In contrast, the behavior at an unsteady state, such as during

Table 2. Fitted parameters of the three models.

Model	K	η_B	n	σ_0	RMSE
HB	2350	–	0.75	3.1	140.3
Bingham	–	1861	–	351.4	209.6
PL	2354	–	0.75	–	128

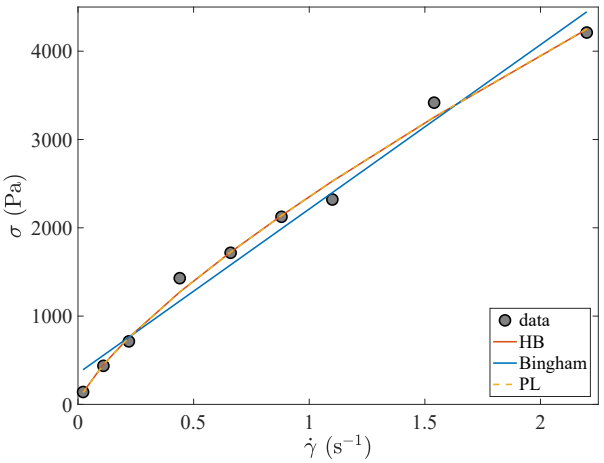

Fig. 5. Relationship between shear stress (σ) and shear rate ($\dot{\gamma}$) at a steady state, fitted to the HB model (red line), Bingham model (blue line), and PL model (dotted yellow line). The model and fitting parameters are listed in **Table 2**.

start-up flow before reaching a steady state, is unsettled. The yield stress is a particularly important parameter for start-up flow and requires further consideration. The behavior may differ from that at a steady state, given that Ishibashi and Sato reported that viscosity decreases with time, even at a constant shear rate [12].

5.3. Microstructural Observations

Figure 6 shows the microstructure of a sample used in a series of rheological measurements at 1180°C. The sample was cut off at a height of 12.6 mm from the base. Microstructures of the cross-section surface are shown in images ④ and ⑤, whereas images ①, ②, and ③ show central areas of the upper part of the sample. The images show that the sample contains homogeneously distributed plagioclase and Fe–Ti oxides. However, the plagioclase is mainly nucleated around the wall of the alumina container, and is not distributed in the molten sample when there is no shearing during crystallization as indicated in **Fig. 7**. Therefore, we consider that the crystals observed in the sample (**Fig. 6**) are efficiently nucleated by shear deformation. This is consistent with a study focused on the effect of deformation rates on crystal kinetics [24], and a study of the shear rate dependent dynamics of basalt solidification [25], which argued that advective processes transport fresh melt to the crystal surface, facilitating growth, when shear is introduced during crystallization. The rheological dependence on shear rate shown

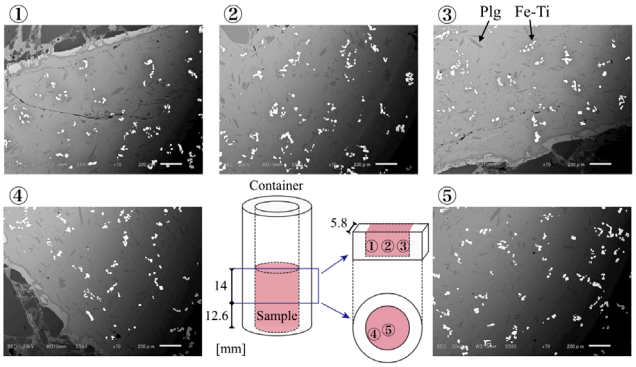

Fig. 6. Back-scattered electron images of a sample quenched at 1180°C and a diagram showing the imaged area of the sample. In the images, the dark gray and elongated rectangles are plagioclase, the white crystals are Fe–Ti oxides, and the background is melt/glass. The outer dark gray area is the alumina crucible container. The white bar at the lower right in each image is a 200 μm scale bar.

in **Figs. 3** and **4**, which is a type of non-Newtonian characteristic, is induced by microstructural variations in the plagioclase and Fe–Ti oxides. The mean crystal volume fraction of 0.14 estimated from back-scattered electron images was sufficient to have caused crystal interactions. In fact, the crystal volume fraction of 0.14 is at approximately the point at which magma starts showing nonlinear rheology in a number of models [6]. Regarding the degree of nonlinearity, previous liquid+crystals models predicted a lower shear thinning for crystal contents of 0.14 [6], while a recent work shows that relative viscosity remarkably increases even at lower crystal content because of the interaction of elongated pyroxene [26]. In this manner, a slight textural change can result in predominant rheological variation and there is so much more to be explored regarding the quantification. In the case of our sample, the interaction between the linearly-distributed Fe–Ti oxide and plagioclase may have caused the strong shear thinning. With respect to the effect of bubbles, the void fraction was less than a few percent inside the sample, thus the bubble effect was negligible [6]. Given that **Fig. 6** shows that the interaction between the alumina container and magmatic sample was limited to the interface, it also does not affect the rheological measurements and overall microstructure of the sample. This highlights the veracity of our experimental apparatus and procedures.

6. Conclusion

This study presents a simple procedure for measuring magma rheology and demonstrated that reliable results can be obtained using this technique. In the measurements, the rheology became non-Newtonian with decreasing temperature, showing clear shear rate dependence together with yield stress. To identify the cause of the non-Newtonian characteristics, we observed the quenched

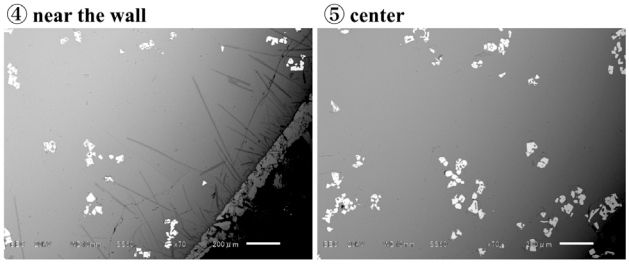

Fig. 7. Back-scattered electron images of a sample quenched at 1180°C without shearing during crystallization. The numbers in the upper left of the images indicate the imaged areas with reference to those in **Fig. 6**. The white bar at the lower right in each image is a 200 μm scale bar.

sample following the experiment. The advantage of our approach is that the sample crucible container is disposable, such that microstructural observations of the entire sample in the container can be undertaken. We examined both horizontal and vertical-section views of the sample and confirmed that crystals of plagioclase and Fe–Ti oxides were nearly uniformly distributed in the quenched sample. The homogeneous crystal distribution was generated by constant shearing during crystallization, resulting in rheological variations because changes in crystal distribution.

Acknowledgements

SEM observations were made at the Geological Survey of Japan, National Institute of Advanced Industrial Science and Technology, with the assistance of N. Geshi and K. Matsumoto. XRF analysis was undertaken by A. Yasuda and N. Hokanishi at the Earthquake Research Institute. M. Nagai helped to sample the lava at Izu–Oshima. We are grateful for their help. This work was supported by the MEXT "Integrated Program for Next Generation Volcano Research and Human Resource Development" and JSPS KAKENHI Grant Number JP 17K14383 to A. K. Kurokawa.

References:

[1] O. Melnik and R. S. J. Sparks, "Controls on conduit magma flow dynamics during lava dome building eruptions," J. of Geophysical Research: Solid Earth, Vol.110, No.B2, B02209, 2005.

[2] L. Caricchi, L. Burlini, P. Ulmer, T. Gerya, M. Vassalli, and P. Papale, "Non-Newtonian rheology of crystal-bearing magmas and implications for magma ascent dynamics," Earth and Planetary Science Letters, Vol.264, No.3-4, pp. 402-419, 2007.

[3] A. Vona, A. D. Piazza, E. Nicotra, C. Romano, M. Viccaro, and D. Giordano, "The complex rheology of megacryst-rich magmas: The case of the mugearitic "cicirara" lavas of Mt. Etna volcano," Chemical Geology, No.458, pp. 48-67, 2017.

[4] M. O. Chevrel, T. Platz, E. Hauber, D. Baratoux, Y. Lavallée, and D. B. Dingwell, "Lava flow rheology: A comparison of morphological and petrological methods," Earth and Planetary Science Letters, Vol.384, pp. 109-120, 2013.

[5] H. Sato, "Viscosity measurement of subliquidus magmas: 1707 basalt of Fuji volcano," J. of Mineralogical and Petrological Sciences, Vol.100, pp. 133-142, 2005.

[6] H. M. Mader, E. W. Llewellin, and S. P. Mueller, "The rheology of two-phase magmas: A review and analysis," J. of Volcanology and Geothermal Research, Vol.257, pp. 135-158, 2013.

[7] J. Engmann and M. R. Mackley, "Semi-solid processing of chocolate and cocoa butter: the experimental correlation of process rheology with microstructure," Food and Bioproducts Processing, Vol.84, No.2, pp. 95-101, 2006.

[8] L. Gilbert, C. Picard, G. Savary, and M. Grisel, "Rheological and textural characterization of cosmetic emulsions containing natural and synthetic polymers: relationships between both data," Colloids and Surfaces A: Physicochemical and Engineering Aspects, Vol.421, pp. 150-163, 2013.

[9] S. Q. Wang, S. Ravindranath, and P. E. Boukany, "Homogeneous shear, wall slip, and shear banding of entangled polymeric liquids in simple-shear rheometry: A roadmap of nonlinear rheology," Macromolecules, Vol.44, pp. 183-190, 2011.

[10] D. B. Dingwell, "Viscosity-temperature relationships in the system Na2Si2O5-Na4Al2O5," Geochimica et Cosmochimica Acta, Vol.50, pp. 1261-1265, 1986.

[11] I. Sonder, B. Zimanowski, and R. Büttner, "Non-Newtonian viscosity of basaltic magma," Geophysical Research Letters, Vol.33, No.2, L02303, 2006.

[12] H. Ishibashi and H. Sato, "Viscosity measurements of subliquidus magmas: Alkali olivine basalt from the Higashi-Matsuura district, Southwest Japan," J. of Volcanology and Geothermal Research, Vol.160, No.3-4, pp. 223-238, 2007.

[13] D. B. Dingwell, "2.15 - Properties of Rocks and Minerals – Diffusion, Viscosity, and Flow of Melts," Treatise on Geophysics: Volume 2, 2nd edition, Elsevier, pp. 419-436, 2015.

[14] H. Ishibashi, "Non-Newtonian behavior of plagioclase-bearing basaltic magma: Subliquidus viscosity measurement of the 1707 basalt of Fuji volcano, Japan," J. of Volcanology and Geothermal Research, Vol.181, No.1-2, pp. 78-88, 2009.

[15] A. Vona, C. Romano, D. B. Dingwell, and D. Giordano, "The rheology of crystal-bearing basaltic magmas from Stromboli and Etna," Geochemica et Cosmochimica Acta, Vol.75, No.11, pp. 3214-3236, 2011.

[16] M. O. Chevrel, C. Cimarelli, L. deBiasi, J. B. Hanson, Y. Lavallée, F. Arzilli, and D. B. Dingwell, "Viscosity measurements of crystallizing andesite from Tungurahua volcano (Ecuador)," Geochemistry, Geophysics, Geosystems, Vol.16, No.3, pp. 870-889, 2015.

[17] A. Kurokawa, M. Takeo, and K. Kurita, "Two types of volcanic tremor changed with eruption style during 1986 Izu-Oshima eruption," J. of Geophysical Research: Solid Earth, Vol.121, No.4, pp. 2727-2736, 2016.

[18] T. Fujii, S. Aramaki, T. Kaneko, K. Ozawa, Y. Kawanabe, and T. Fukuoka, "Petrology of the Lavas and Ejecta of the November, 1986 Eruption of Izu-Oshima Volcano," Bulletin of the Volcanological Society of Japan, Vol.33, pp. S234-S254, 1988 (in Japanese with English abstract).

[19] S. Aramaki and T. Fujii, "Petrological and Geological Model of 1986-1987 Eruption of Izu-Oshima Volcano," Bulletin of the Volcanological Society of Japan, Vol.33, pp. S297-S306, 1988 (in Japanese with English abstract).

[20] F. J. Spera, A. Borgia, J. Strimple, and M. Feigenson, "Rheology of melts and magmatic suspensions: 1. Design and calibration of concentric cylinder viscometer with application to rhyolitic magma," J. of Geophysical Research: Solid Earth, Vol.93, No.B9, pp. 10273-10294, 1988.

[21] D. B. Dingwell and D. Virgo, "Viscosities of melts in the Na2O-FeO-Fe2O3-SiO2 system and factors controlling relative viscosities of fully polymerized silicate melts," Geochimica et Cosmochimica Acta, Vol.52, No.2, pp. 395-403, 1988.

[22] D. Giordano, J. K. Russell, and D. B. Dingwell, "Viscosity of magmatic liquidus: A model," Earth and Planetary Science Letters, Vol.271, No.1-4, pp. 123-134, 2008.

[23] F. Vetere, S. Rossi, O. Namur, D. Morgavi, V. Misiti, P. Mancinelli, M. Petrelli, C. Pauselli, and D. Perugini, "Experimental constraints on the rheology, eruption, and emplacement dynamics of analog lavas comparable to Mercury's northern volcanic plains," J. of Geophysical Research: Planets, Vol.122, No.7, pp. 1522-1538, 2017.

[24] A. Vona and C. Romano, "The effects of undercooling and deformation rates on the crystallization kinetics of Stromboli and Etna basalts," Contributions to Mineralogy and Petrology, Vol.166, No.2, pp. 491-509, 2013.

[25] S. Kolzenburg, D. D. Genova, D. Giordano, K. U. Hess, and D. B. Dingwell, "The effect of oxygen fugacity on the rheological evolution of crystallizing basaltic melts," Earth and Planetary Science Letters, Vol.487, pp. 21-32, 2018.

[26] F. Vetere, H. Sato, H. Ishibashi, R. D. Rosa, and P. Donato, "Viscosity changes during crystallization of a shoshonitic magma: new insights on lava flow emplacement," J. of Mineralogical and Petrological Sciences, Vol.108, No.3, pp. 144-160, 2013.

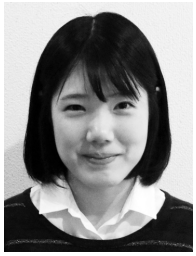

Name:
Aika K. Kurokawa

Affiliation:
Associated Research Fellow, National Research Institute for Earth Science and Disaster Resilience (NIED)

Address:
3-1 Tennodai, Tsukuba, Ibaraki 305-0006, Japan

Brief Career:
2016- Associated Research Fellow, National Research Institute for Earth Science and Disaster Resilience (NIED)

Selected Publications:
• "Rheological behavior of water-ash mixtures from Sakurajima and Ontake volcanoes: implications for lahar flow dynamics," Bulletin of Volcanology, Vol.80, No.6, Article 50, 2018.

Academic Societies & Scientific Organizations:
• Volcanological Society of Japan (VSJ)
• American Geophysical Union (AGU)

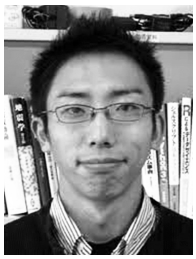

Name:
Takahiro Miwa

Affiliation:
Researcher, National Research Institute for Earth Science and Disaster Resilience (NIED)

Address:
3-1 Tennodai, Tsukuba, Ibaraki 305-0006, Japan

Brief Career:
2010 Postdoctoral, Geological Survey of Japan
2011 COE Fellow, Tohoku University
2013 Postdoctoral, Kyushu University
2014- National Research Institute for Earth Science and Disaster Resilience (NIED)

Selected Publications:
• "Resuspension of ash after the 2014 phreatic eruption at Ontake volcano, Japan," J. of Volcanology and Geothermal Research, Vol.351, pp. 105-114, 2018.

Academic Societies & Scientific Organizations:
• Volcanological Society of Japan (VSJ)
• American Geophysical Union (AGU)

Name:
Hidemi Ishibashi

Affiliation:
Associate Professor, Department of Geoscience, Faculty of Science, Shizuoka University

Address:
836 Ohya, Suruga-ku, Shizuoka 422-8529, Japan

Brief Career:
2007- Project Researcher, Institute for Geothermal Sciences, Kyoto University
2008- Project Researcher, Geochemical Research Center, The University of Tokyo
2011- Project Researcher, Earthquake Research Institute, The University of Tokyo
2012- Department of Geoscience, Faculty of Science, Shizuoka University

Selected Publications:
• "Non-Newtonian behavior of plagioclase-bearing basaltic magma!′ Subliquidus viscosity measurement of the 1707 basalt of Fuji volcano, Japan," J. of Volcanology and Geothermal Research, Vol.181, pp. 78-88, 2009.
• "Ultra-magnesian olivine-bearing ultramafic lava blocks within Cenozoic accretionary sediments at Shizuoka, Japan: Implications for young, hot plume activity beneath the western Pacific Plate," Lithos, Vol.324-325, pp. 315-324, 2019.

Academic Societies & Scientific Organizations:
• Volcanological Society of Japan (VSJ)
• Japan Association of Mineralogical Sciences (JAMS)
• American Geophysical Union (AGU)